Preprints of the 10th IFAC International Symposium on Dynamics and Control of Process Systems
The International Federation of Automatic Control
December 18-20, 2013. Mumbai, India

On the Tuning of Predictive Controllers for Hybrid Fuel Cell Vehicle Applications ⋆

Syed K. Ahmed * **Donald J. Chmielewski** **

* *email: ahmesye5@iit.edu*
** *Corresponding author:phone: 312-567-3537, email: chmielewski@iit.edu*

Abstract: While the notion of a hybrid fuel cell vehicles is conceptually promising, due to an off-loading of peak power demands from the fuel cell to the storage devices, the questions of device coordination is unsettled. Clearly the prominent role of equipment limitations, with respect to energy storage capacity and maximum power, suggests the use of predictive control for constraint enforcement. In this work an MPC tuning method specifically tailored to the hybrid vehicle application is presented. The approach is based on the notion of backed-off operating point selection and has the objective of minimizing energy losses from the storage devices. In addition, a soft constraint formulation unique to hybrid vehicle application is proposed.

1. INTRODUCTION

The subject of control system design for hybrid vehicles has enjoyed much attention in the recent literature (see the overview papers Salmasi (2007); Opila et al. (2009); Sciarretta and Guzzella (2007)). The basic idea is to use the fuel cell as the primary source of energy. However, to meet large power demands, the fuel cell will be hybridized with one or more energy storage devices. Consider the case of an acceleration event. Rather than quickly ramp up the power output of the fuel cell - and potentially damage its internal components - one could turn to a supercapacitor for the short burst of power. Then, over the subsequent time period, a smaller increase in fuel cell power output would recharge the capacitor. This configuration will also allow for regenerative braking.

If given such a configuration, a fundamental question concerns the coordination of power output from each device. How much power should each device provide in response to a demand? How fast should a storage device be recharged and to what level? If the system contains more than one storage technology - each with unique power/energy density characteristics - then the issue becomes even more complicated. Central to the power coordination question is the physical limits of each device. Clearly, a battery or supercapacitor can hold only a finite amount of energy and cannot output power if the reserve is fully depleted. In addition, the rate of charging and discharging of these devices should be limited to observe heat dissipation related safety concerns. Similarly, a fuel cell will have a maximum power output limit and cannot accept any power. In addition, one may wish to limit the ramp rate of fuel cell power output, in an effort to reduce degradation rates.

Clearly, the presence of equipment limitations suggests the use of Model Predictive Control (MPC). Unfortunately, the tuning of such a controller is unexpectedly challenging and non-intuitive. Thus, the objective of this paper is to present an MPC tuning method that not only provides the type of response expected from a hybrid system, but also yields minimum energy loss. The outline of the paper is as follows. The next section provides a brief introduction to MPC, while Section 3 presents the high level system model of the hybrid fuel cell vehicle. Then, the method of statistically constrained controller design is presented as the first step of the tuning procedure. In Section 5, the linear feedback of the statistically constrained controller is converted to an MPC structure for enforcement of point-wise-in-time constraints.

2. REVIEW OF MPC

The basic idea behind MPC is to utilize a dynamic model to make predictions about performance about the future [1]. Based on these predicted outcomes, the manipulated variable at the present time will be selected. Then, in the next time-step, new measurement information will be fed back to the model and a new set of predicted outcomes will be calculated. To highlight the predictive aspect of MPC, two time indices are utilized. The index k is for predictions, while the index i represents actual time. Specifically, the sequence $x(k|i), \quad k = i \ldots i + N$ is the state prediction at time i. Thus, a linear predictive model with horizon N can be compactly stated as

$$x(k+1|i) = A_d x(k|i) + B_d u(k|i) \tag{1}$$

$$z(k|i) = D_x x(k|i) + D_u u(k|i) \tag{2}$$

$$z^{min} \le z(k|i) \le z^{max} \qquad k = i..i + N - 1 \tag{3}$$

$$x(i|i) = x(i) \tag{4}$$

where $x, u,$ and z are the state, manipulated and performance vectors, z^{min} and z^{max} are the output constraints and $x(i)$ is the state of the actual system at time i. The first objective of MPC is to select a sequence, $u(k|i), \quad k = i \ldots i + N - 1$, such that all of the predicted performance

⋆ Center for Electrochemical Science & Engineering, Department of Chemical & Biological Engineering, Illinois Institute of Technology, Chicago, IL 60616

[1] For a detailed description of MPC please see Cutler and Ramaker (1980); Garcia et al. (1989); Rawlings (1999, 2000); Qin and Badgwell (2003).

outputs satisfy the constraints $z^{min} \le z(k|i) \le z^{max} \quad k = i \ldots, i+N-1$. In most cases, there will be more than one sequence $u(k|i)$ capable of satisfying the output constraints. To alleviate this issue the sequence selection process is cast as an optimization problem. This optimization will typically have a quadratic objective function

$$\sum_{k=i}^{i+N-1} \begin{bmatrix} x(k|i) \\ u(k|i) \end{bmatrix}^T \begin{bmatrix} Q & M \\ M^T & R \end{bmatrix} \begin{bmatrix} x(k|i) \\ u(k|i) \end{bmatrix}$$
$$\ldots + x(i+N|i)^T P x(i+N|i) \tag{5}$$

The weights Q, R and M are constants that must be selected such that the compound matrix is at least positive semidefinite (see Russell (1979) for additional restrictions) and P is usually selected as the solution to the Ricatti equation (Chmielewski and Manousiouthakis, 1996)

$$P = A_d^T P A_d + Q \quad \ldots$$
$$-(A_d^T P B_d + M)(B_d^T P B_d + R)^{-1}(B_d^T P A_d + M^T) \tag{6}$$

Another important issue is the existence of a feasible sequence $u(k|i)$. That is, there could be values of $x(i)$ such that all sequences $u(k|i)$ will result in some constraint violation. In this case, all sequences will be invalid, but the controller will still need to provide a numeric input to the process. To address this concern, a soft constraint formulation of MPC is usually employed (Zheng and Morari (1995)). The basic procedure is to introduce a vector of slack variables $\theta \ge 0$. Then, the original 'hard' constraints are replaced by the following soft constraints $z^{min} - \theta \le z(k|i) \le z^{max} + \theta$. Finally, a weighted sum of the slack variables, $c_\theta^T \theta$, is added to the MPC objective function. Then, if the elements of c_θ are set to sufficiently large values, the optimization will select $\theta \simeq 0$, except for the cases in which the hard constraints would be infeasible. That is, the constraints of controller are relaxed, $\theta > 0$, only if the optimization has no other choice. In summary, the optimization solved within a soft constrained MPC is the following

$$\min_{\substack{x(k|i)\\ u(k|i)\\ z(k|i),\theta}} \left\{ \sum_{k=i}^{i+N-1} \begin{bmatrix} x(k|i) \\ u(k|i) \end{bmatrix}^T \begin{bmatrix} Q & M \\ M^T & R \end{bmatrix} \begin{bmatrix} x(k|i) \\ u(k|i) \end{bmatrix} \atop \ldots + x(i+N|i)^T P x(i+N|i) + c_\theta^T \theta \right\}$$

$$\begin{aligned} s.t.\ & x(k+1|i) = A_d x(k|i) + B_d u(k|i) \\ & z(k|i) = D_x x(k|i) + D_u u(k|i) \\ & z^{min} - \theta \le z(k|i) \le z^{max} + \theta \qquad k = i \ldots i+N-1 \\ & x(i|i) = x(i) \end{aligned}$$

If the solution to this problem is denoted as $u^*(k|i)$, then the manipulated input given to the process at time i is $u(i) = u^*(i|i)$. The feedback aspect of this controller resides in the initial condition $x(i)$. Specifically, at the next time-step a new set of process measurements will become available and an updated initial condition $x(i+1)$ will be generated. With this new value in place, a new solution to the optimization will be calculated and used to define the next manipulated input: $u(i+1) = u^*(i+1|i+1)$.

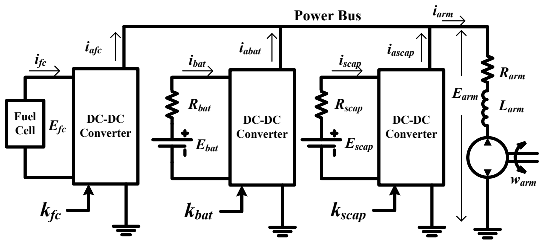

Fig. 1. Canonical hybrid vehicle power system

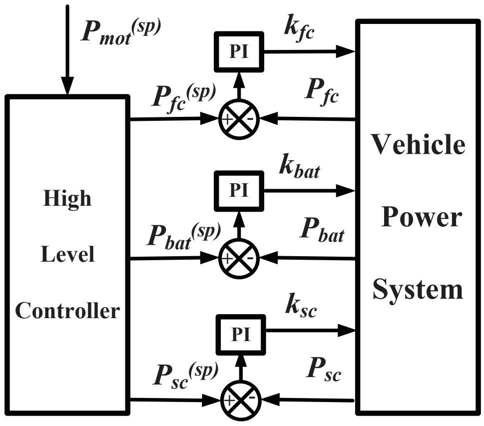

Fig. 2. Hybrid vehicle controller hierarchy

3. HYBRID FUEL CELL VEHICLE MODEL

To illustrate the method a system consisting of two storage devices (a battery and a supercapacitor) and a fuel cell will be used. A high level model of this system is summarized as follows (Ahmed and Chmielewski, 2012) :

$$\dot{E}_{bat} = -P_{bat} - P_{bat}^{(loss)}, 0 \le E_{bat} \le E_{bat}^{max}, |P_{bat}| \le P_{bat}^{max} \tag{7}$$
$$\dot{E}_{sc} = -P_{sc} - P_{sc}^{(loss)}, 0 \le E_{sc} \le E_{sc}^{max}, |P_{sc}| \le P_{sc}^{max} \tag{8}$$
$$\dot{P}_{fc} = \Delta P_{fc}, 0 \le P_{fc} \le P_{fc}^{max}, |\Delta P_{fc}| \le \Delta P_{fc}^{max} \tag{9}$$

where $E_{bat}, E_{sc}, P_{bat}, P_{sc}$ are energy within and power out of the battery and super capacitor, $P_{fc}, \Delta P_{fc}$ is the fuel cell power and its ramp rate, $P_i^{(loss)} = P_i^2/\hat{L}_i$, are power losses ($i = bat, sc$), and E_{bat}^{max}, E_{sc}^{max}, P_{fc}^{max}, P_{bat}^{max}, P_{sc}^{max}, ΔP_{fc}^{max} are the device limits.

Table 1. Disturbance Model Parameters

i	$\tau_i(s)$	$\bar{w}_i(W)$	$S_{w_i}(kW^2 \cdot s)$
l	4.3×10^4	162	4354
m	909	18	92
h	5	0	884

The power requested by the operator and sent to the motor is modeled by the following shaping filter.

$$P_{mot} = P_l + P_m + P_h \tag{10}$$
$$\dot{P}_l = (w_l - P_l)/\tau_l \tag{11}$$
$$\dot{P}_m = (w_m - P_m)/\tau_m \tag{12}$$
$$\dot{P}_h = (w_h - P_h)/\tau_h \tag{13}$$

where each w_i is stationary white noise with mean $\bar{w}_i$ and spectral density S_{w_i} ($i = l, m, h$). The parameters of this model are given in Table 1. The basic idea is that P_l

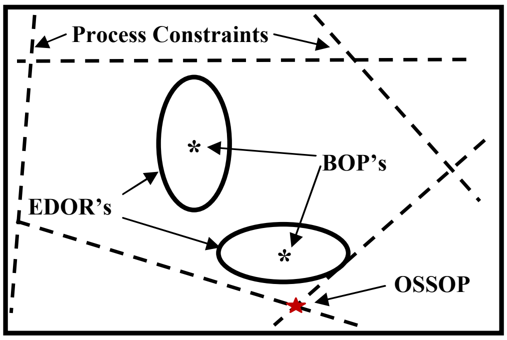

Fig. 3. The economics of back-off selection

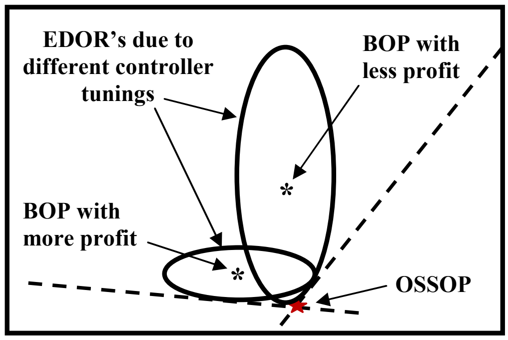

Fig. 4. BOP selection and controller design

will capture the low frequency aspects of power demand, P_m will capture the medium frequency aspects and P_h represents the high frequency aspects. It is highlighted that the disturbance model of Equation(10)-(13), is to be used only for controller design, though we also use it for our simulations. In the actual system, P_{mot} will be a received signal from the vehicle operator.

Finally, a power balance between the three devices and the motor yields the following equality that must be enforced at all times:

$$P_{mot} = P_{fc} + P_{bat} + P_{sc} \tag{14}$$

A linearized model in deviation variables with respect to the time-averaged conditions is as follows. $\dot{x} = Ax + Bu + Gw$, $z = D_x x + D_u u$, $z^{min} \leq z \leq z^{max}$, where $x = s - \bar{s}$, $u = m - \bar{m}$, $w = w - \bar{w}$, $z = q - \bar{q}$, $z^{min} = q^{min} - \bar{q}$, $z^{max} = q^{max} - \bar{q}$, $s = [E_{bat}\ E_{sc}\ P_{fc}\ P_l\ P_m\ P_h]^T$, $m = [P_{sc}\ \Delta P_{fc}]$, $w = [w_l\ w_m\ w_h]^T$, $q = [E_{bat}\ E_{sc}\ P_{fc}\ P_{bat}\ P_{sc}\ \Delta P_{fc}]^T$ and $\bar{s}$, $\bar{m}$, $\bar{w}$, $\bar{q}$ are the time-averaged values of s, m, w, and q. The matrices A, B, G, D_x, D_u, and S_w are given below.

$$A = \begin{bmatrix} 0 & 0 & 1 & -1 & -1 & -1 \\ 0 & 0 & 0 & 0 & 0 & 0 \\ 0 & 0 & 0 & 0 & 0 & 0 \\ 0 & 0 & 0 & -1/\tau_l & 0 & 0 \\ 0 & 0 & 0 & 0 & -1/\tau_m & 0 \\ 0 & 0 & 0 & 0 & 0 & -1/\tau_h \end{bmatrix} \quad B = \begin{bmatrix} 1 & 0 \\ -1 & 0 \\ 0 & 1 \\ 0 & 0 \\ 0 & 0 \\ 0 & 0 \end{bmatrix} \tag{15}$$

$$G = \begin{bmatrix} 0 & 0 & 0 \\ 0 & 0 & 0 \\ 0 & 0 & 0 \\ 1/\tau_l & 0 & 0 \\ 0 & 1/\tau_m & 0 \\ 0 & 0 & 1/\tau_h \end{bmatrix} \quad S_w = \begin{bmatrix} S_{w_l} & 0 & 0 \\ 0 & S_{w_m} & 0 \\ 0 & 0 & S_{w_h} \end{bmatrix} \tag{16}$$

$$D_x = \begin{bmatrix} 1 & 0 & 0 & 0 & 0 & 0 \\ 0 & 1 & 0 & 0 & 0 & 0 \\ 0 & 0 & 1 & 0 & 0 & 0 \\ 0 & 0 & -1 & 1 & 1 & 1 \\ 0 & 0 & 0 & 0 & 0 & 0 \\ 0 & 0 & 0 & 0 & 0 & 0 \end{bmatrix} \quad D_u = \begin{bmatrix} 0 & 0 \\ 0 & 0 \\ 0 & 0 \\ -1 & 0 \\ 1 & 0 \\ 0 & 1 \end{bmatrix} \tag{17}$$

Using the sample and hold method (Burl, 1999) with a sample time of 0.5 s the model of (1)-(3) is determined.

4. STATISTICALLY CONSTRAINED CONTROL SYSTEM DESIGN

The proposed design scheme is based on the notion of back-off control. The basic idea is that one would like to operate at the Optimal Steady-State Operating Point (OSSOP), typically at a corner of the feasible operating region (see Figure 3). However, operation at the OSSOP is impossible due to the influence of external disturbances. These disturbances will cause the system to operate, not at a single point, but within an Expected Dynamic Operating Region (EDOR). If one attempts to operate at the OSSOP, the EDOR will almost certainly extend beyond the constraint set and result in numerous violations. Thus, the challenge is to select a Backed-off Operating Point (BOP) that is economically close to the OSSOP (to maximize profit) while ensuring that the EDOR is completely contained within the constraint set (to avoid violations). While EDOR size and shape is a function of the disturbances acting on the process, the selected control system will have a strong influence. This ability to manipulate the EDOR can then be used to reduce the amount of back-off (see Figure 4).

Using a full state information structure, the controller is assumed to be of the following linear feedback form: $u(i) = Lx(i)$, where the gain matrix L is selected such that statistical interpretations of the output constraints are enforced. Specifically, the controller must be such that two times the standard deviation of each output is less than the distance between the time-averaged value of the output and the constraint limit:

$$2\sigma_i < q_i^{max} - \bar{q}_i \quad \text{and} \quad 2\sigma_i < \bar{q}_i - q_i^{min} \qquad i = 1 \ldots, 6 \tag{18}$$

The standard deviation of each output is calculated as:

$$\Sigma_x = (A_d + B_d L)\Sigma_x (A_d + B_d L)^T + G_d \Sigma_w G_d^T \tag{19}$$

$$\zeta_i = \rho_i \left[(D_x + D_u L)\Sigma_x (D_x + D_u L)^T \right] \rho_i^T \tag{20}$$

$$\sigma_i = \sqrt{\zeta_i} \quad i = 1 \ldots, 6 \tag{21}$$

where ρ_i is the ith row of an identity matrix.

In general, the time-averaged values of each output (the $\bar{q}_i$'s) can be selected freely. However, they must satisfy the following condition:

$$\bar{q}_3 + \bar{q}_4 + \bar{q}_5 = \bar{P}_{mot} \tag{22}$$

where $\bar{P}_{mot} = \bar{w}_l + \bar{w}_m + \bar{w}_h$. To account for thermal losses the time averaged power of each storage device is required to equal the time averaged loss:

$$\bar{q}_4 = -(\bar{q}_4^2 + \sigma_4^2)/\hat{L}_{bat}$$
$$\bar{q}_5 = -(\bar{q}_5^2 + \sigma_5^2)/\hat{L}_{sc}$$

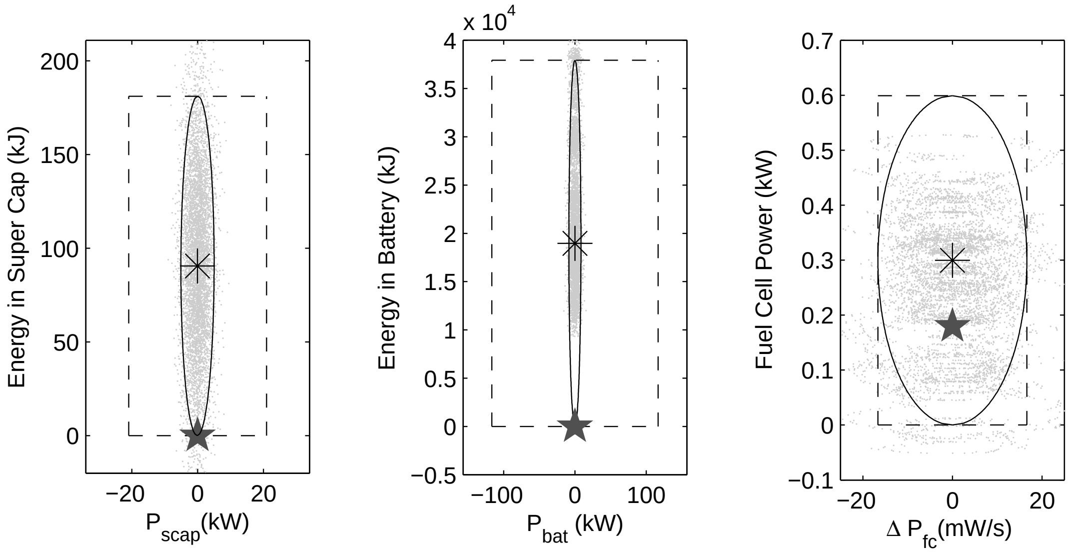

Fig. 5. Optimal Back-off, EDOR and scatter plot resulting from simulation of statistically constrained controller

Table 2. Parameter Table

Parameter	Value	Units
E_{bat}^{max}	3.79×10^4	kJ
E_{sc}^{max}	181.4	kJ
P_{fc}^{max}	0.599	kW
P_{bat}^{max}	116.7	kW
P_{sc}^{max}	20.99	kW
ΔP_{fc}^{max}	16.64	mW/s
$\hat{L}_{bat}$	5.36	kW
$\hat{L}_{sc}$	197.47	kW

If these equality constraints are relaxed to inequalities, they may be converted to the following Linear Matrix Inequalities

$$\begin{bmatrix} -\bar{q}_4 & \bar{q}_4 & \sigma_4 \\ \bar{q}_4 & \hat{L}_{bat} & 0 \\ \sigma_5 & 0 & \hat{l}_{bat} \end{bmatrix} > 0 \quad \begin{bmatrix} -\bar{q}_5 & \bar{q}_5 & \sigma_5 \\ \bar{q}_5 & \hat{L}_{sc} & 0 \\ \sigma_5 & 0 & \hat{L}_{sc} \end{bmatrix} > 0 \tag{23}$$

To ensure the above relaxations are (near) active, the following inequality is introduced

$$\bar{P}_{loss} > -\bar{q}_4 - \bar{q}_5 \tag{24}$$

In summary, the statistically constrained controller design problem is defined as:

$$\min_{\bar{P}_{loss},\bar{q}_i,L,\Sigma_x,\zeta_i,\sigma_i} \bar{P}_{loss} \tag{25}$$
$$s.t. \quad Equations\ (18) - (24)$$

Using the parameters of Table 1 and Table 2, and the computational methods presented of Peng et al. (2005), the solution to the Problem (25) was found to be:

$$L = \begin{bmatrix} -0.0045 & 15.5 & -12.1 & 4.7 & 28.4 & 396 \\ 0 & 0 & -0.45 & 0.14 & 0.0044 & 0 \end{bmatrix} 10^{-3} \tag{26}$$

The optimal BOP is depicted in Figure 5 (the * points) along with the OSSOP (the pentagram points). Figure 5 also depicts the two standard deviation EDORs as the solid line ellipses. The energy, power, and ramp rate constraints are depicted as the dashed lines. The scatter plot points are a simulation using the shaping filter to generate P_{mot}. Clearly, there is a statistical enforcement of the constraints. The loss of power can be found in the fuel cell plot, as the difference between the time-averaged fuel cell power, 300 W (the BOP), and the time-averaged motor power, 180 W (the OSSOP).

5. MPC TUNING

The conversion of the linear statistically constrained controller to MPC form should be such that the EDOR of the resulting MPC is similar to the original linear feedback. To begin the conversion consider the following unconstrained version of MPC

$$\min_{x(k|i),u(k|i)} \left\{ \begin{array}{c} \sum_{i=k}^{i+N-1} \begin{bmatrix} x(k|i) \\ u(k|i) \end{bmatrix}^T \begin{bmatrix} Q & M \\ M^T & R \end{bmatrix} \begin{bmatrix} x(k|i) \\ u(k|i) \end{bmatrix} \\ \cdots + x(i+N|i)^T P x(i+N|i) \end{array} \right\}$$
$$x(k+1|i) = A_d x(k|i) + B_d u(k|i)$$
$$x(i|i) = x(i)$$

Then, for an arbitrary selection of Q, R, and M such that the compound matrix is positive definite and P is set equal to the positive definite solution of Equation 6, it is well known that the feedback policy generated by the unconstrained MPC will be identical to $u(i) = L_{LQR}x(i)$ The subscript LQR highlights the fact that this controller is of the Linear Quadratic Regulator class:

$$L_{LQR} = (B_d^T P B_d + R)^{-1}(B_d^T P A_d + M) \tag{27}$$

This observation leads to the following conversion strategy. Given the linear feedback suggested by the statistically constrained controller design scheme, find quadratic objective weights Q, R, and M such that the unconstrained MPC will generate a policy identical to the original. The first issue in this strategy concerns the existence of such weights. This question is answered in Peng et al. (2005), where a class of controller design problem (of which (25) is a member) are shown to generate linear controllers in the LQR family. The second issue of constructing suitable weights is addressed by the following theorem, from Chmielewski and Manthanwar (2004):

Theorem 1: If $P > 0$ and $R > 0$ s.t.

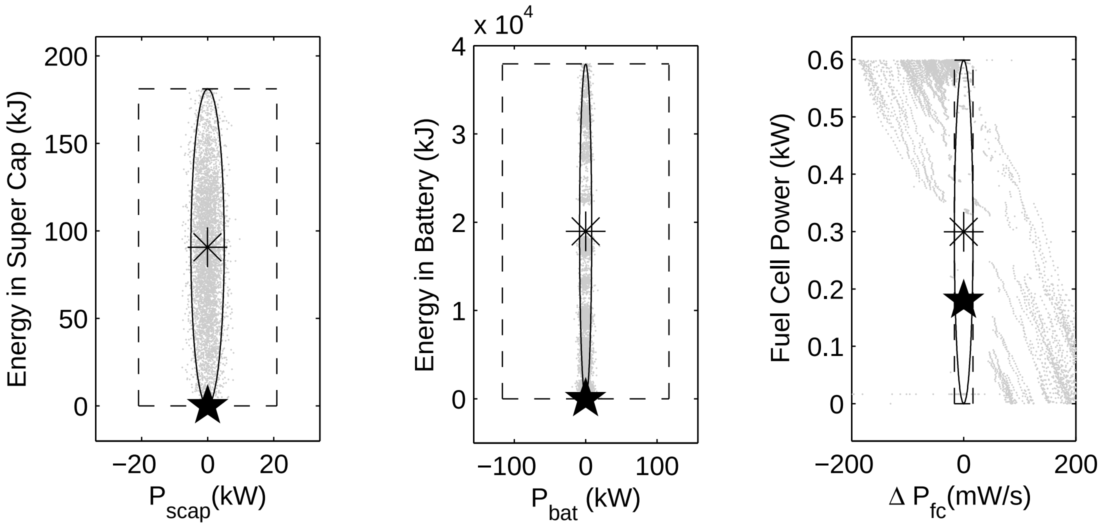

Fig. 6. Scatter plot from simulation of MPC Controller

$$\begin{bmatrix} P - A_d^T P A_d + L^T(R + B_d^T P B_d)L & L^T(R + B_d P B_d)^T + A_d^T P B_d \\ (R + B_d^T P B_d)L + B_d^T P A_d & R \end{bmatrix} > 0 \tag{28}$$

then $Q = P - A_d^T P A_d + L^T(R + B_d^T P B_d)L$ and $M = L^T(R + B_d^T P B_d) + A_d^T P B_d$ will be s.t.

$$\begin{bmatrix} Q & M \\ M^T & R \end{bmatrix} > 0 \tag{29}$$

and P and L will satisfy (6) and (27).

Application of Theorem 1 to the gain of Eqn (26) results in the following quadratic objective function weights:

$$Q = \begin{bmatrix} 0 & 0 - 0.0004 & 0.0001 & -0.0001 & -0.0010 & \\ 0 & 0.293 & 3.08 & -0.753 & 0.503 & 7.220 \\ -0.0004 & 3.076 & 32.4 & -7.95 & 5.28 & 75.8 \\ 0.0001 & -0.753 & -7.95 & 1.95 & -1.29 & -18.57 \\ -0.0001 & 0.503 & 5.28 & -1.29 & 0.863 & 12.4 \\ -0.0010 & 7.22 & 75.83 & -18.57 & 12.39 & 177.9950 \end{bmatrix} \tag{30}$$

$$R = \begin{bmatrix} 17.33 & 25.6 \\ 25.6 & 190 \end{bmatrix} \tag{31}$$

$$M = \begin{bmatrix} 0.0008 & 0.0012 \\ -2.70 & -3.98 \\ 2.21 & 3.95 \\ -0.86 & -1.48 \\ -4.93 & -7.28 \\ -68.5 & -101 \end{bmatrix} \tag{32}$$

It is highlighted that the mapping from the controller to objective function weights is not unique and results are expected to very depending on the LMI solver used. The important test is to check if the obtained weights generate an LQR controller equal to the original.

The next question concerns the impact of re-imposing output constraints on the MPC formulation. As illustrated in Section 4, the unconstrained MPC is designed to statistically observe the output constraints. Thus, if point-wise-in-time constraints are imposed, then one would expect these constraints to be active only a small fraction of the time, assuming the actual disturbance has characteristics equal to the disturbance model.

The next step is to construct the soft constraint structure. This begins by ranking the constraints by order of importance. The least important are those on the fuel cell ramp rate. While a violation of these constraints will reduce cell life, there is no safety or hardware limitation. The next set are the constraints on the battery and supercapacitor power. While there is a safety concern it is physically possible to violate these constraints. The last set are those for which the equipment dictates that a violation is impossible. This includes fuel cell power and energy within the storage devices. As such slack variables were defined only for the fuel cell ramp rate and power of the two storage devices ($\theta = [\theta_{\Delta P_{fc}} \quad \theta_{bat} \quad \theta_{sc}]^T$) and the soft constraint weights were selected to reflect the relative importance of each.

Unfortunately, simulation with this limited set of soft constraints will eventually result in the MPC becoming infeasible. This is due to the fact that the energy storage limits cannot be softened. For example, if both the battery and supercapacitor are out of energy, the fuel cell is will unlikely be able to make up the difference. Similarly, if both storage devices are full then regenerative braking will be impossible. One option is to restructure the slack variables. Specifically, the power balance is redefined as

$$P_{mot} = P_{fc} + P_{sc} + P_{bat} + \theta_{unav} - \theta_{fric} \tag{33}$$

where both, θ_{unav} and θ_{fric}, are required to be positive and possess heavy linear weights in the objective function. The impact is expected to be as follows. If the power request, P_{mot}, is larger than the three devices can deliver due to E_{sc} and E_{bat} being zero, then θ_{unav} will become positive to make the problem feasible. However, the operator will see this as unavailable power in the amount θ_{unav}. Similarly, if regenerative braking is active ($P_{mot} < 0$) and neither of the two storage devices can take any more power, then θ_{fric} will become active and send this power to the friction brake.

Figures 6 illustrates the performance of constrained MPC. Clearly the occurrence of constraint violations is virtually eliminated. The exception is in the ΔP_{fc} direction where we see significant utilization of the slack variable. The time series plots of Figure 7 gives a more detailed account of the soft constraints. At 16.4 minutes the super-capacitor reaches its maximum energy limit and P_{sc} is forced to be zero or positive. (Note that based on the definition of P_{sc}, a positive value indicates a discharging of the battery). At the same time the ΔP_{fc} slack variable becomes active and allows P_{fc} to quickly move to zero. At 17.2 minutes, both storage devices reach their maximum energy limits and the friction brake must become active.

ACKNOWLEDGEMENTS

Financial support provided by the National Science Foundation (CBET - 0967906) and the STAR fellowship provided by the Graduate College at the Illinois Institute of Technology.

REFERENCES

S. Ahmed and D.J. Chmielewski. Power system and controller design for hybrid fuel cell vehicles: Conceptual development. *IEEE Transactions on Control System Technology, Submitted*, 2012.

J.B. Burl. *Linear optimal control: H_2 and H_∞ methods.* Addison Wesley Longman (Menlo Park, Calif.), 1999.

D. Chmielewski and V. Manousiouthakis. On constrained infinite-time linear quadratic optimal control. *Systems & Control Letters*, 29(3):121–129, 1996.

D.J. Chmielewski and A.M. Manthanwar. On the tuning of predictive controllers: Inverse optimality and the minimum variance covariance constrained control problem. *Ind. Eng. Chem. Res*, 43 (24):7807–7814, 2004.

C.R. Cutler and B.L. Ramaker. Dynamic matrix control—a computer control algorithm. In *Proceedings of the Joint Automatic Control Conference, San Francisco*, 1980.

C.E. Garcia, D.M. Prett, and M. Morari. Model predictive control: Theory and practice–a survey* 1. *Automatica*, 25(3):335–348, 1989.

D.F. Opila, X. Wang, R. McGee, J.A. Cook, and JW Grizzle. Performance comparison of hybrid vehicle energy management controllers on real-world drive cycle data. In *American Control Conference, 2009. ACC'09.*, pages 4618–4625. IEEE, 2009.

J.K. Peng, A.M. Manthanwar, and D.J. Chmielewski. On the tuning of predictive controllers: The minimum back-off operating point selection problem. *Ind. Eng. Chem. Res*, 44(20):7814–7822, 2005.

S.J. Qin and T.A. Badgwell. A survey of industrial model predictive control technology. *Control engineering practice*, 11(7):733–764, 2003.

J.B. Rawlings. Tutorial: Model predictive control technology. In *American Control Conference, 1999. Proceedings of the 1999*, volume 1, pages 662–676. IEEE, 1999.

J.B. Rawlings. Tutorial overview of model predictive control. In *Control Systems, IEEE*, volume 20, 3, pages 38–52. IEEE, 2000.

D.L. Russell. *Mathematics of Finite Dimensional Control Systems*. Lecture Notes in Pure and Applied Mathematics. Marcel Dekker, 1979. ISBN 9780824772116.

F.R. Salmasi. Control strategies for hybrid electric vehicles: Evolution, classification, comparison, and future trends. *Vehicular Technology, IEEE Transactions on*, 56(5):2393–2404, 2007. ISSN 0018-9545.

A. Sciarretta and L. Guzzella. Control of hybrid electric vehicles. *Control Systems Magazine, IEEE*, 27(2):60–70, 2007. ISSN 0272-1708.

A. Zheng and M. Morari. Stability of model predictive control with mixed constraints. *Automatic Control, IEEE Transactions on*, 40 (10):1818–1823, 1995.

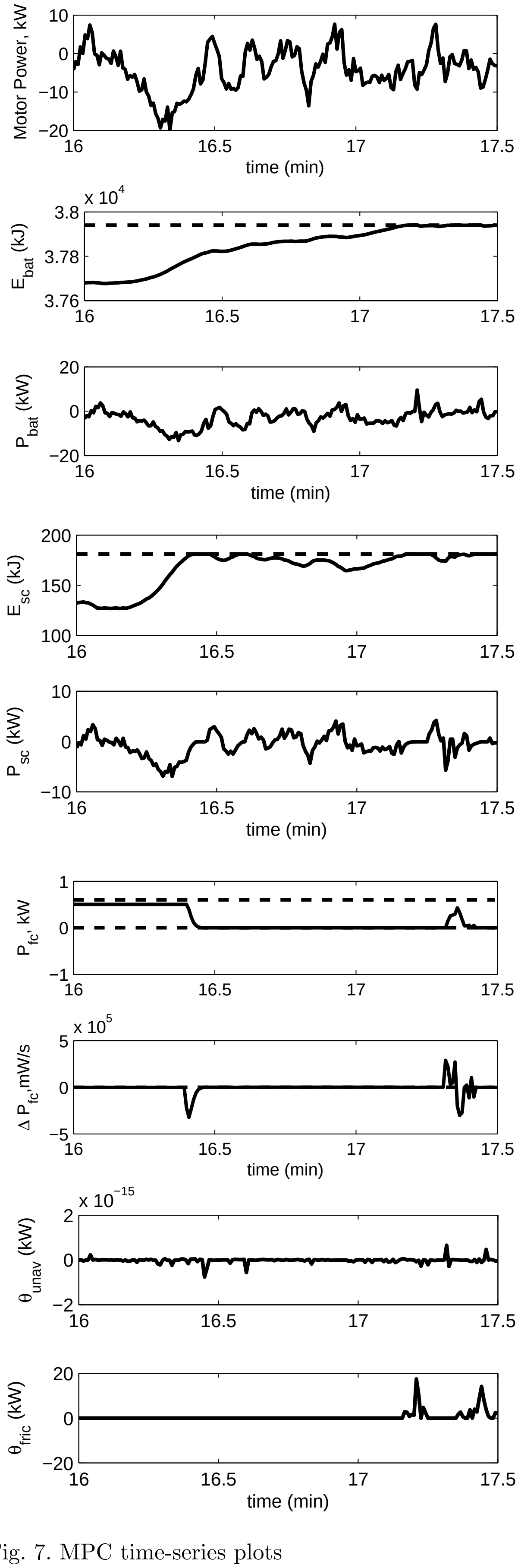

Fig. 7. MPC time-series plots